Rapid Expansion Nozzles for Gas Dynamic Lasers

R. A. GREENBERG,* A. M. SCHNEIDERMAN,† D. R. AHOUSE,‡ AND E. M. PARMENTIER §
Avco Everett Research Laboratory, Everett, Mass.

A rapid expansion nozzle is a critical feature of a gas dynamic laser, since the nozzle freezes the vibrational energy of the working gas, allowing a population inversion to be obtained downstream. The amount of vibrational energy frozen in the expansion is controlled by the size and shape of the nozzle. This paper discusses the influence of these parameters on the performance of a GDL. Two aspects of the problem are presented. The first is a quantitative shock tunnel investigation of the flow in GDL nozzles utilizing a laser interferometer. The second is a detailed analysis of the influence of these flows on the available vibrational energy in the lasing cavity. Both sharp and rounded transonic nozzle contours were investigated. All of these nozzles exhibit smooth transition to supersonic flow without regions of flow separation.

Introduction

A RAPID expansion nozzle is a critical feature of a gas dynamic laser (GDL), because the nozzle freezes the vibrational energy of the working gas, allowing a population inversion to be obtained downstream as illustrated in Fig. 1 (Ref. 1). Therefore, the performance of a GDL is influenced by the rate of expansion of the gases through the nozzle. The parameter which characterizes the performance of a nozzle is the ratio of the flow transit time through the nozzle to the appropriate vibrational relaxation time. The former can be varied by either changing the characteristic dimension of the nozzle, i.e., its throat height, or its shape; the latter is essentially fixed by the stagnation conditions of the working gas. In this paper, we will be concerned with the effects of nozzle shape and size on the performance of a GDL.

As shown in Fig. 2, GDL nozzles typically consist of a row of blades, each containing a subsonic inlet, a transonic throat, and a supersonic expansion contour. The most rapid two-dimensional supersonic expansion is a centered Prandtl-Meyer expansion fan originating from a sharp corner located at the minimum area. If the flow is restricted to two dimensions, the rate of the expansion within the corner expansion fans is governed only by the throat height, and is independent of the final corner angle. For this reason, significant decreases in flow transit time through a nozzle of fixed throat height and area ratio can only be achieved by minimizing the time spent in the subsonic-transonic flow. Therefore, the primary emphasis of this work involves the influence of rapid subsonic expansion on GDL performance.

The experimental work was performed by obtaining interferograms of the nozzle flowfields in a shock tunnel at gas conditions appropriate to GDL operation. The interferograms portray the entire density field in the nozzle in great detail. This information yields the density distribution along the nozzle centerline and wall streamlines directly, and with appropriate assumptions (i.e., streamline coordinates), can give the density distribution along all streamlines of the flow. Since the purpose here was to evaluate the influence of the fluid mechanics on the kinetic performance of the nozzles, the experimental density distributions along the centerlines were used in computations of the vibrationally nonequilibrium flow. Thus the kinetic performance of the various contours could be compared to determine the influence of the various geometric parameters on the amount of vibrational energy frozen by the nozzle.

A variety of subsonic nozzle contours was investigated to determine the extent of the performance gain which could be achieved. The parameters which were varied included the subsonic inlet angle and the radius of curvature of the nozzle at the throat. The range of these parameters which were investigated included conventional wind tunnel nozzle designs, e.g., 30° inlet semi-angle with a three throat height radius of curvature, and unconventional designs, e.g., 90° inlet semi-angle with a sharp corner at the throat. Further details of this work can be found in Ref. 2.

Experimental Apparatus

A conventional 6-in. diam shock tunnel was used as the gas supply for the nozzle studies. The area ratio of the nozzle was large enough so that it appeared as a slightly leaky end wall to the incident shock. The shock tunnel operated with a driver mixture of 90% He, 10% N_2 and a driven mixture of 83% N_2, 16% CO_2, one percent H_2, with initial driver and driven pressures selected to give the desired flow conditions. A nominal stagnation temperature and pressure of 1200°K and 2 atm, with a test time

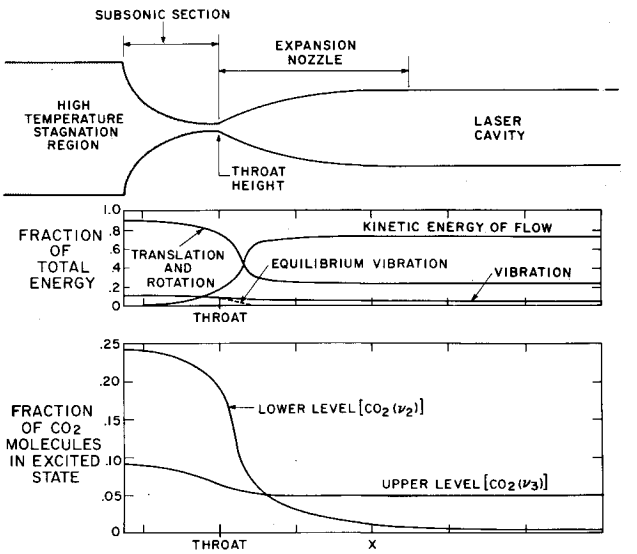

Fig. 1 Operating principles of a gas dynamic laser.

Presented as Paper 72-148 at the AIAA 10th Aerospace Sciences Meeting, San Diego, Calif., January 17-19, 1972; submitted January 31, 1972; revision received June 19, 1972. This research was supported by the Air Force Weapons Laboratory, Air Force Systems Command, United States Air Force, Kirtland Air Force Base, N. Mex. and Advanced Research Projects Agency, ARPA Order 870 under Contract F29601-69-C-0060.

Index categories: Lasers; Nozzles and Channel Flow; Subsonic and Transonic Flow.

* Principal Research Engineer. Associate Fellow AIAA.
† Principal Research Scientist. Member AIAA.
‡ Senior Scientist.
§ Scientist.

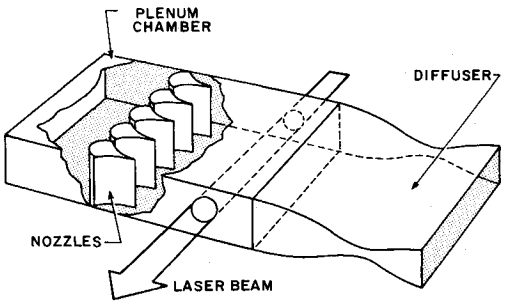

Fig. 2 Schematic of a gas dynamic laser.

of approximately 1 msec, was obtained. Diagnostics included pressure transducers for measurement of stagnation pressure and static pressure. The initial shock speed, (determined with a series of thin film heat-transfer gages), was used, along with the initial pressure, to compute the stagnation pressure. This pressure agreed with the measured stagnation pressure very well.

The family of nozzle contours which was investigated is shown in Table 1. The dimensions of the contours are scaled by the throat height. The density distributions in these nozzles were obtained with the Mach-Zender interferometer shown in Fig. 3 which uses a neon laser light source.[3-5] The laser operates at 5401 Å, and generates 10 kw, 3 nsec pulses at up to 100 pulses/sec. The laser coherence length is 30 cm.

Results

Interferograms obtained from three nozzles, representing the extremes in subsonic geometry encompassed by the present experiment, are shown in Figs. 4a, 4b, and 4c. Referring to Table 1, they are contours 1, 5 and 3. This selection exhibits the two qualitative features observed in all nozzle geometries tested. First, both the subsonic and supersonic flows were aerodynamically clean, i.e., no regions of separated flow or strong shocks were present. Nozzle contour 3 therefore demonstrates the most rapid possible subsonic expansion while still achieving the required degree of flow uniformity. Second, for the nozzles with nonzero throat radius of curvature the transonic flowfield was surprisingly close to one-dimensional. The one-dimensionality of the transonic flow is possibly the result of two compensating effects; sink flow and transonic nozzle curvature. Concave

	θ_1	$\bar{R} = \frac{R}{h}$	θ_2
1.	45°	3	5°
2.	45°	1	5°
3.	90°	0	90°
4.	90°	1	5°
5.	45°	0	45°
6.	26°	3	0°
7.	20°	PARABOLIC	0°

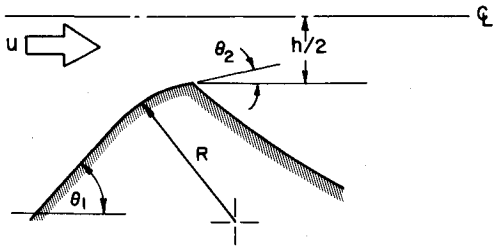

Table 1 Nozzle geometries tested

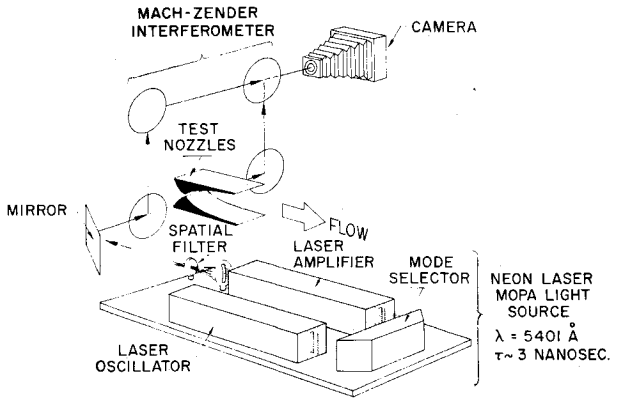

Fig. 3 Schematic of laser interferometer.

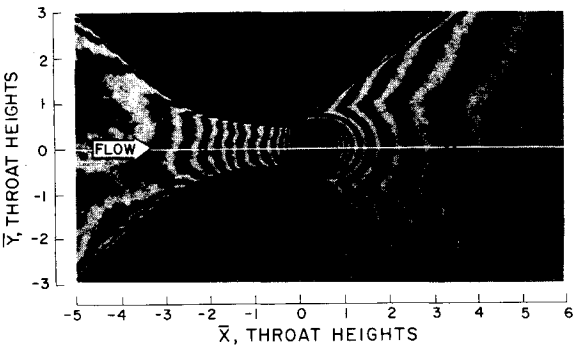

Fig. 4a Interferogram of contour 1 ($\bar{R} = 3$, $\theta_1 = 45°$, $\theta_2 = 5°$).

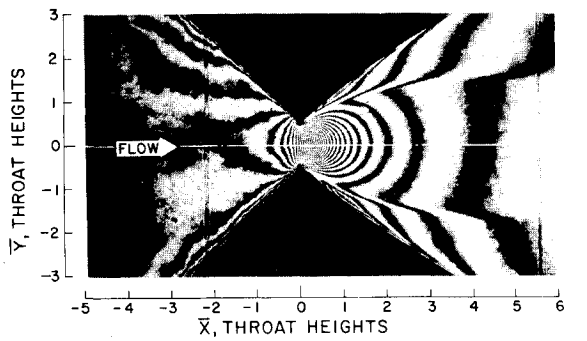

Fig. 4b Interferogram of contour 5 ($\bar{R} = 0$, $\theta_1 = 45°$, $\theta_2 = 45°$).

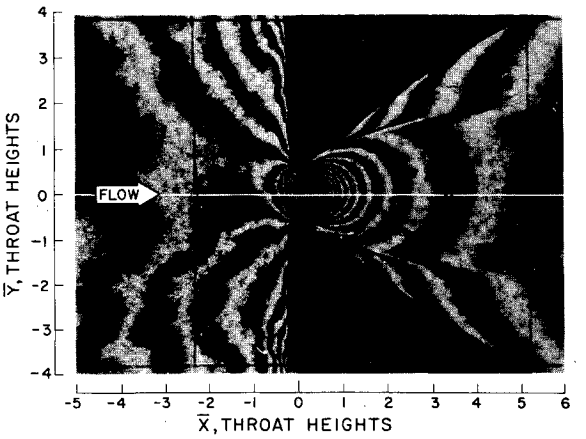

Fig. 4c Interferogram of contour 3 ($\bar{R} = 0$, $\theta_1 = 90°$, $\theta_2 = 90°$).

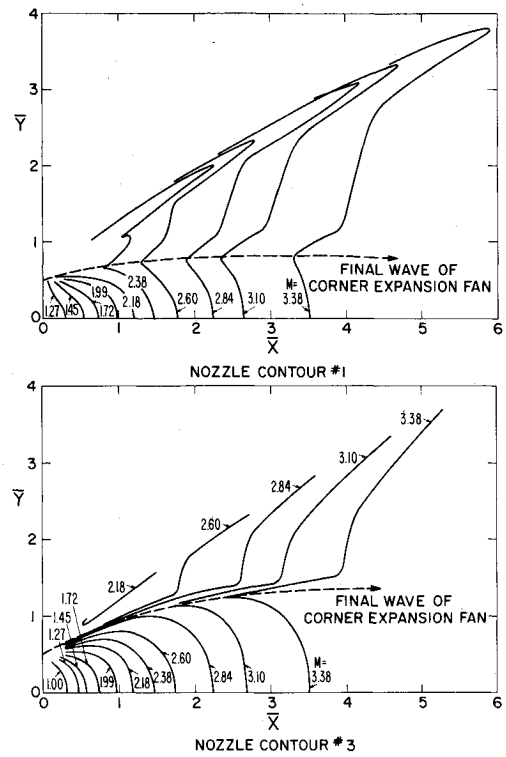

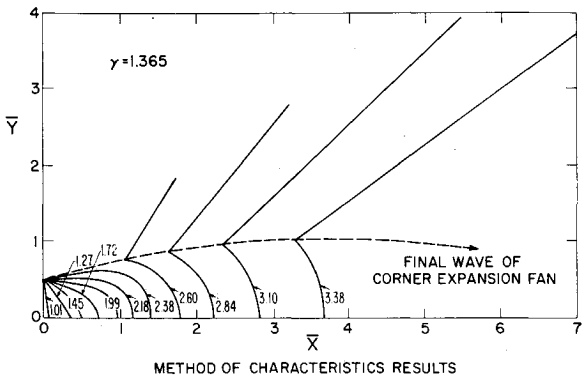

Fig. 5 Comparison of theoretical and experimental constant property lines.

curvature of the nozzle in the transonic region tends to accelerate the off axis flow more rapidly than the centerline flow producing a curvature of the constant property lines in the flow direction. Conversely, sink flow will tend to accelerate the centerline flow more rapidly than the off axis flow producing a curvature of the opposite sense. Thus, as the flow passes from the subsonic inlet into the curved portion of the nozzle it passes from a region dominated by sink flow to a region dominated by transonic curvature. The resulting interaction produces a flow which is nearly one-dimensional.

Examination of the interferograms in Figs. 4b and 4c indicates that the supersonic expansion fan is terminated by a weak shock wave, with a strength of 1 or 2%. This phenomenon is explored

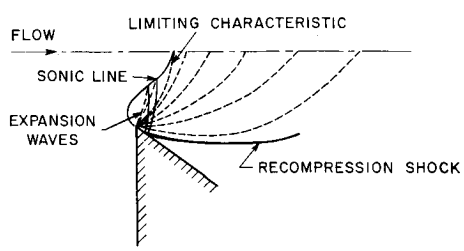

Fig. 6 Sketch of transonic flow at sharp corner (contour 3).

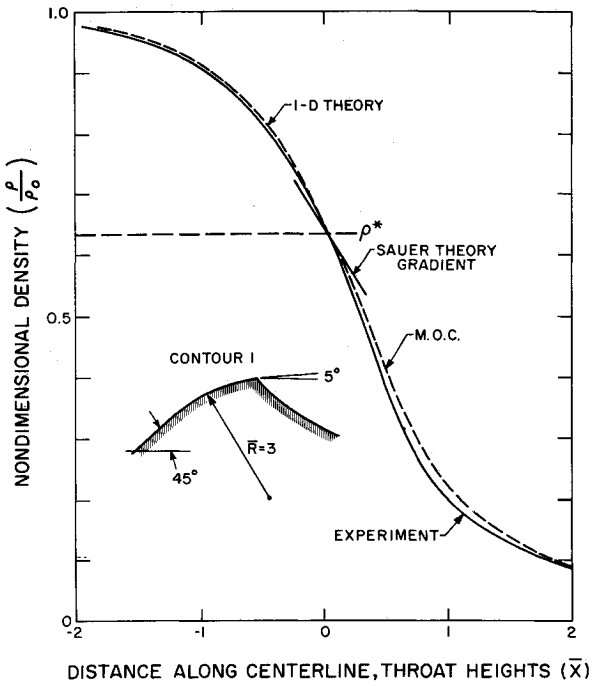

Fig. 7a Comparison of experimental and theoretical centerline density profiles for contour 1.

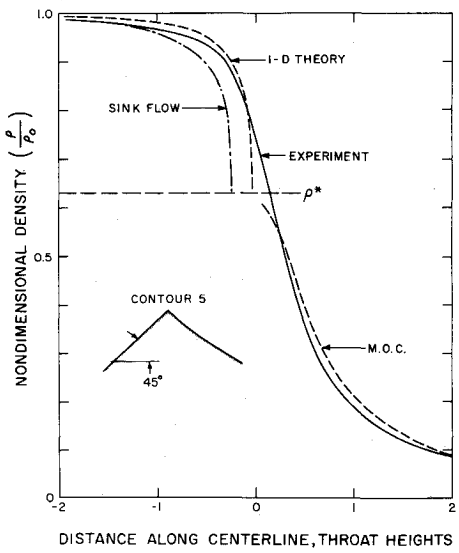

Fig. 7b Comparison of experimental and theoretical centerline density profiles for contour 5.

further in Figs. 5 and 6. Figure 5 shows lines of constant Mach number and the location of the final wave of the expansion fan as predicted by the method of characteristics along with experimental results obtained from the interferograms. The theoretical calculations assume uniform flow with a straight sonic line at the nozzle throat. The final wave of the expansion fan in contour 3 is downstream of the position predicted by the theory, indicating that the flow is the overexpanded and then recompressed by the shock.

A possible explanation of the origin of this overexpansion followed by a recompression is sketched in Fig. 6. Close examination of the transonic portions of the interferograms shows that the sonic line is shaped roughly as shown in this figure. The flow near the corner starts its supersonic expansion before it is parellel to the axis of the nozzle. This causes the flow to overexpand downstream of the corner. Also, there is a small region of transonic flow between the sonic line and the limiting characteristic where the expansion waves from the sharp corner can reflect from the sonic line. Since the sonic line is a constant

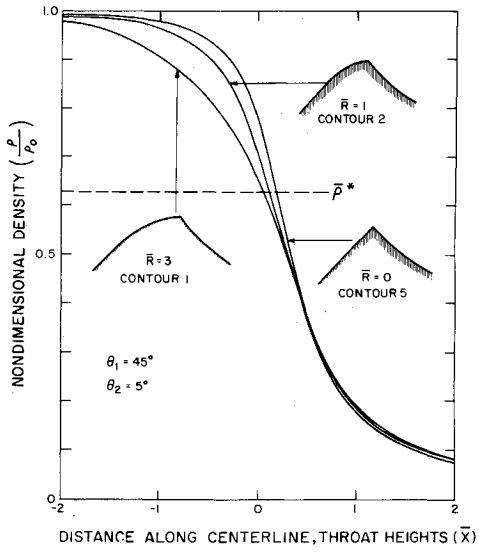

Fig. 8 Influence of subsonic curvature on centerline density profiles.

pressure line, the expansion waves are reflected as compression waves. These waves cross the expansion fan and are reflected from the nozzle just downstream of the corner, coalesce to form a weak shock, and propagate downstream into the supersonic flow where they terminate the expansion fan. This shock is so weak that it does not influence the gas kinetics of the laser.

The centerline density profiles obtained from the interferograms of Figs. 4a and 4b are presented in Figs. 7a and 7b. One-dimensional theory predictions using $\gamma = 1.365$ for the subsonic flow and method of characteristics predictions for the supersonic flow are included for comparison with the experimental data. Also included in Fig. 7a is a sonic point density gradient calculated using the theory of Sauer[6] and in Fig. 7b a density profile calculated from compressible sink flow.

One-dimensional calculations agreed with all of the measured profiles to within $\pm 5\%$, except for contour 5. For this nozzle the extreme subsonic geometry resulted in a considerable departure from one-dimensional predictions. The transonic flowfield was confined to the region of the supersonic corner expansion which is a highly two-dimensional flowfield. Qualitatively, the deviations between the one-dimensional calculations and the experimental profiles for the remaining contours are in part explainable by sink flow and subsonic curvature effects.

The point of sink flow influence is further emphasized in Fig. 7b. The subsonic contour under consideration in this figure, nozzle 5, contains no curvature and, as such, permits a meaningful compressible sink flow calculation to be made. Up to a distance of one throat height from the geometric nozzle throat, the sink flow results show better agreement with the experimental data than the one-dimensional results. Near the throat, the influence

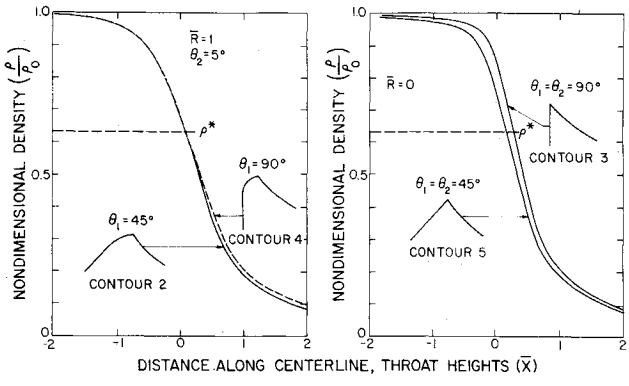

Fig. 9 Influence of subsonic entrance angle on centerline density profiles.

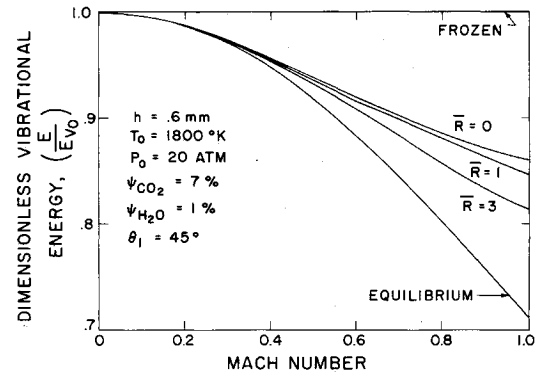

Fig. 10 Effect of contour radius of curvature on vibrational freezing.

of the sharp corner expansion is dominant and the sink flow model becomes inappropriate.

To determine the influence of the remaining subsonic geometric variables on the measured centerline density profiles, selective composite plots of the data were made. The first of these, presented in Fig. 8, shows the influence of subsonic curvature. Included are profiles for $\bar{R}$ equal to three, one, and zero. The three profiles graphically illustrate the trends observed in Fig. 7. As the radius of curvature decreases, the transonic density gradients become larger. However, the most important point to note from Fig. 8 is that changing $\bar{R}$ from one to zero does not significantly alter the density gradients in the nozzle.

For a limited variation in subsonic inlet angle, θ_1, it was possible to separate the influence of θ_1 and θ_2 (the inlet angle to the supersonic expansion) on the nozzle centerline density profiles. Shown in Fig. 9 are two sets of curves for θ_1 equal to 45° and 90°. In the set on the left curvature is present while on the right it is not. For the case with curvature present with the θ_2 fixed at 5°, no perceptible change in density can be observed with changes in θ_1. For the case with no curvature and θ_1 equal to θ_2, changing θ_1 from 45° to 90° causes a horizontal translation

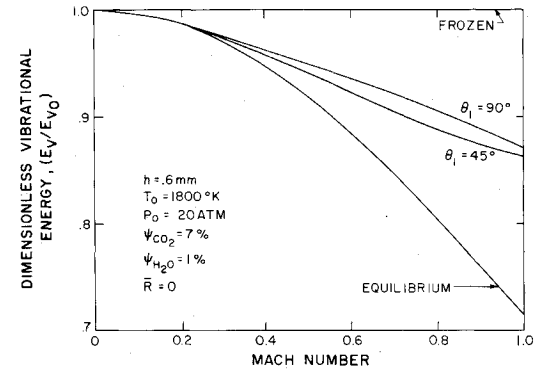

Fig. 11 Effect of entry angle on vibrational freezing.

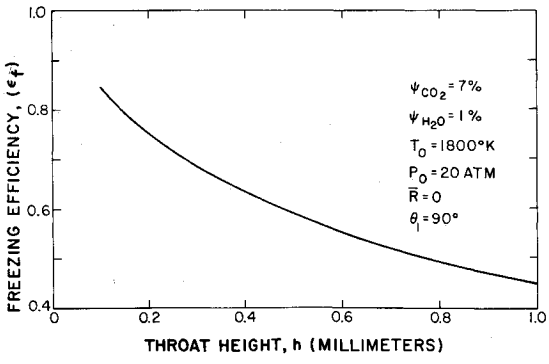

Fig. 12 Variation of freezing parameter with nozzle throat height for inviscid flow.

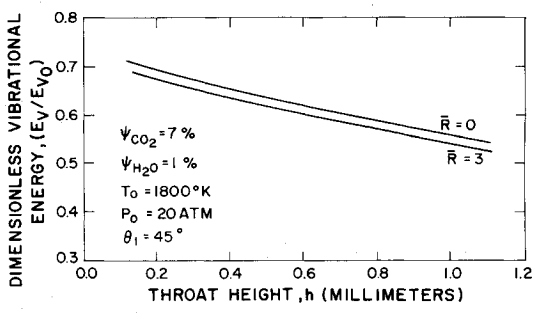

Fig. 13 Vibrational energy frozen 20 cm downstream of the nozzle throat of an area ratio 25 nozzle.

in ρ/ρ_0 but does not distort it in any other way. Therefore the influence of θ_1 on the density gradients in these nozzles is very small.

Kinetics

The freezing efficiency of various subsonic contours has been determined by calculating the vibrational relaxation of an initially excited gas along the nozzle center streamline. The mole fraction in the gas mixture considered were 7% CO_2, 1% H_2O, and 92% N_2. Of greatest interest in present applications are the CO_2 (v_3) and N_2 vibrational modes. A stagnation temperature of 1800°K and a stagnation pressure of 20 atm were assumed. Pressure distributions along the nozzle center streamlines were obtained from the measured densities by assuming the flow to be frozen at an effective γ of 1.365.

The vibrational relaxation along the center streamline of the subsonic flow was calculated using the analysis of Ref. 7. In this analysis rotational and translational equilibrium is assumed, and each of the vibrational modes is modeled as an equilibrium harmonic oscillator. Vibration of v_1, v_2, and v_3 modes of CO_2, v_2 of H_2O, and N_2 are considered. For a specified pressure distribution along a streamtube, all other flow properties, Mach number, translational temperature, vibrational energies, etc. were calculated.

Figures 10 and 11 show the vibrational energy of the CO_2 (v_3) and N_2 modes per molecule of the mixture as a function of Mach number along the nozzle centerline. These are compared in each case to the equilibrium vibrational energy distribution which depends not on the pressure distribution along the nozzle centerline, but only on the local pressure. The equilibrium distribution plotted vs Mach number is then the same for all the nozzle contours.

Figure 10 compares nozzle contours of various radii of curvature. Decreasing the radius of curvature increases the fraction of vibrational energy remaining at the end of the subsonic section of the nozzle. The contour with $\bar{R} = 0$ represents the maximum possible energy frozen for the given throat height, stagnation conditions, and gas composition. Figure 11 shows the effect of increasing nozzle entry angle with all other geometric variables remaining fixed. The gas is accelerated faster for higher entry angles and hence a larger fraction of the vibrational energy is frozen.

The amount of vibrational energy frozen in the subsonic flows of the nozzle contours may be summarized in terms of a parameter, ε_f, defined as

Table 2 Subsonic freezing parameter at a stagnation pressure of 20 atm

h	$\bar{R}$	θ_1	ε_f(%)
0.6 mm	0	90°	55.
	0	45°	52.
	1	45°	47.
	3	45°	36.

$$\varepsilon_f = \frac{(E_v/E_{v_0})_{M=1} - (E_v/E_{v_0})^{M=1}_{\text{equilibrium}}}{1 - (E_v/E_{v_0})^{M=1}_{\text{equilibrium}}}$$

The equilibrium case represents the least possible fraction of vibrational energy remaining at the nozzle throat, while the frozen case represents the maximum possible fraction of vibrational energy remaining, i.e., all the stagnation energy is frozen. Hence ε_f is the fraction of the largest possible increase in energy frozen attainable from improved subsonic freezing. The numerical values of ε_f are given in Table 2. The contour radius of curvature, $\bar{R}$ is seen to have the largest effect on ε_f. The effect of entry angle, at least for the case of $\bar{R} = 0$, is small. The entry angle affects the acceleration of the gas only at very low Mach numbers where the temperature remains nearly equal to the stagnation temperature and the degree of vibrational nonequilibrium is small.

The variation of ε_f with throat height has been calculated for the contour with $\bar{R} = 0$ and a 90° entry angle, and is plotted in Fig. 12. The effect of nozzle boundary layers is not included, however, it is estimated to significantly influence ε_f for throat heights less than approximately 0.1 mm.

Figure 13 presents results of additional calculations performed to assess the effects of changes in throat height on vibrational energy in the CO_2 (v_3) and N_2 vibration downstream of the supersonic expansion, at a location 20 centimeters from the nozzle exit. For $\bar{R} = 0$, subsonic pressures on the nozzle centerline are again obtained from experimental data, but for $\bar{R} = 3$ the subsonic flow is assumed one-dimensional and the subsonic contour is a circular arc. For the same amount of vibrational freezing, the $\bar{R} = 0$ contour allows the use of significantly larger throat heights. For a fixed device size, the number of nozzles required varies inversely with the nozzle throat height.

References

[1] Gerry, E. T., "Gasdynamic Lasers," *Laser Focus*, Vol. 6, No. 12, Dec. 1970.

[2] Greenberg, R. A., Schneiderman, A. M., Ahouse, D. R. and Parmentier, E. M., "Rapid Expansion Nozzles for Gas Dynamic Lasers," AMP 314, Dec. 1970, Avco Everett Research Lab.

[3] Schneiderman, A. and Itzkan, I., "Interferometric Gas Flow Studies with a Pulsed Neon Laser," *Journal of Applied Physics*, Vol. 41, No. 5, April 1970.

[4] Leonard, D. A., Neal, R. A. and Gerry, E. T., "Observation of a Superradiant Self-Terminating Green Laser Transition in Neon," *Applied Physics Letters*, Vol. 7, No. 6, Sept. 1965.

[5] Leonard, D. A., Caristi, R. F. and Szoke, A., private communication.

[6] Sauer, R., "General Characteristics of the Flow Through Nozzles at Near Critical Speeds," TM 1147 1947, NACA.

[7] Wood, A. D., Camac, M. and Gerry, E. T., "Effects of 10.6 Micron Laser Induced Air Chemistry on Atmospheric Refraction Index," Research Rept. 350, July 1970, Avco Everett Research Lab.